


RESEARCH

Open Access



CRRT circuit venous air chamber design and intra-chamber flow dynamics: a computational fluid dynamics study

Kota Shimizu¹, Toru Yamada², Kazuhiro Moriyama^{3*} , China Kato², Naohide Kuriyama⁴, Yoshitaka Hara⁴, Takahiro Kawaji⁴, Satoshi Komatsu⁴, Yohei Morinishi², Osamu Nishida⁴ and Tomoyuki Nakamura⁴

Abstract

Background Venous air trap chamber designs vary considerably to suit specific continuous renal replacement therapy circuits, with key variables including inflow design and filter presence. Nevertheless, intrachamber flow irregularities do occur and can promote blood coagulation. Therefore, this study employed computational fluid dynamics (CFD) simulations to better understand how venous air trap chamber designs affect flow.

Methods The flow within a venous air trap chamber was analyzed through numerical calculations based on CFD, utilizing large eddy simulation. The working fluid was a 33% glycerin solution, and the flow rate was set at 150 ml/min. A model of a venous air trap chamber with a volume of 15 ml served as the computational domain. Calculations were performed for four conditions: horizontal inflow with and without a filter, and vertical inflow with and without a filter. Streamline plots and velocity contour plots were generated to visualize the flow.

Results In the horizontal inflow chamber, irrespective of filter presence, ultimately the working fluid exhibited a downstream vortex flow along the chamber walls, dissipating as it progressed, and being faster near the walls than in the chamber center. In the presence of a filter, the working fluid flowed uniformly toward the outlet, while in the absence of a filter the flow became turbulent before reaching the outlet. These observations indicate a streamlining effect of the filter.

In the vertical inflow chamber, irrespective of filter presence, the working fluid flowed vertically from the inlet into the main flow direction. Part of the working fluid bounced back at the chamber bottom, underwent upward and downward movements, and eventually flowed out through the outlet. Stagnation was observed at the top of the chamber. Without a filter, more working fluid bounced back from the bottom of the chamber.

Conclusions CFD analysis estimated that the flow in a venous air trap chamber is affected by inflow method and filter presence. The “horizontal inflow chamber with filter” was identified as the design creating a smooth and uninterrupted flow throughout the chamber.

Keywords Computational fluid dynamics, Computational fluid dynamics analysis, Continuous renal replacement therapy, Grid diagram, Horizontal inflow chamber, Streamlines of the flow field, Velocity contours of the flow field, Venous air trap chamber, Vertical inflow chamber, Working fluid

*Correspondence:

Kazuhiro Moriyama
anbix55@gmail.com

Full list of author information is available at the end of the article



© The Author(s) 2024. **Open Access** This article is licensed under a Creative Commons Attribution 4.0 International License, which permits use, sharing, adaptation, distribution and reproduction in any medium or format, as long as you give appropriate credit to the original author(s) and the source, provide a link to the Creative Commons licence, and indicate if changes were made. The images or other third party material in this article are included in the article's Creative Commons licence, unless indicated otherwise in a credit line to the material. If material is not included in the article's Creative Commons licence and your intended use is not permitted by statutory regulation or exceeds the permitted use, you will need to obtain permission directly from the copyright holder. To view a copy of this licence, visit <http://creativecommons.org/licenses/by/4.0/>. The Creative Commons Public Domain Dedication waiver (<http://creativecommons.org/publicdomain/zero/1.0/>) applies to the data made available in this article, unless otherwise stated in a credit line to the data.

Background

In global markets, a variety of continuous renal replacement therapy (CRRT) machines are available, each featuring its own unique design. As an integral part of a CRRT circuit, the venous air trap chamber captures air and clots from the blood to prevent their ingress into the body [1, 2]. The structure of this chamber is adapted to the circuit's needs and may differ in terms of inflow method, presence of filters, chamber capacity, shape, and other parameters. Nevertheless, in clinical practice, clot formation within the venous air trap chamber is sometimes experienced [3]. Specifically, the chamber's filters are believed to impact the occurrence of blood coagulation, because they may induce turbulence and cause the blood flow to stagnate [4]. Such coagulation may not only lead to system downtime and insufficient blood purification [5, 6], but also to potential blood loss for the patient [7]. Therefore, designing a venous air trap chamber that promotes a smooth blood flow is expected to help prevent blood coagulation. Regarding venous air trap chamber design evaluation, there have been in vitro studies on bubble removal efficiency [1, 2] and clinical studies on the association with thrombus formation [4]. However, to the best of our knowledge, there have only been a few reports that quantitatively evaluated how differences in chamber design can affect the flow within the venous air trap chamber [8, 9].

In the present study, we quantitatively estimated and visualized the flow within a venous air trap chamber by using computational fluid dynamics (CFD) simulations, and hereby evaluated the impact of differences in chamber design.

Materials and methods

Analysis methods

The flow in a venous air trap chamber model was estimated and visualized using numerical calculations based on CFD. CFD is a method to simulate various flow conditions and provides many advantages, including a higher degree of freedom in addressing flow and a more detailed information compared with experimental settings. It has been used to evaluate various flow fields not only of engineering applications but also of vascular systems [10, 11], and is well established as a simulation tool to predict various fluid flow phenomena. In CFD, the working fluid is first defined, and then governing equations are determined and discretized. Next, the computational domain is defined and discretized (grid division). Numerical calculations are then performed, and finally, analysis and evaluation are conducted on the basis of the numerical data.

Definition of working fluid

The working fluid refers to the fluid under analysis, and, in this study, was a 33% glycerin solution (density: 1.071 g/cm³, viscosity: 1.876 mPa s at 37°C) flowing within the venous air trap chamber. This solution is commonly used to simulate blood [12–14]. Additionally, the working fluid was defined to flow steadily into the venous air trap chamber from the inlet at a flow rate of 150 ml/min, while the flow rate at the outlet was the same as that at the inlet, based on the law of conservation of mass. For both inlet and outlet boundaries, the velocities were set to be uniform.

Selection and discretization of governing equations

In this study, we selected the large eddy simulation (LES) method to simulate the fluid flow in the venous air trap chamber to efficiently model the unsteady turbulence behavior in the venous air trap chamber and capture its effect on the flow field. This method is shown to be sufficiently reliable by our results, which demonstrate large velocity fluctuations owing to turbulence production generated by the large velocity gradient of the jet flow at the inlet side. The governing equations for LES are based on the filtered continuity equation and the Navier–Stokes equations. The continuity equation and Navier–Stokes equations describe the conservation of mass and momentum, respectively, and in the context of LES for incompressible flows, they are expressed as:

$$\frac{\partial \bar{u}_i}{\partial x_i} = 0 \quad (1)$$

$$\frac{\partial \bar{u}_i}{\partial t} + \frac{\partial \bar{u}_i \bar{u}_j}{\partial x_j} = -\frac{\partial \bar{P}}{\partial x_i} + \frac{\partial}{\partial x_j} \left[(\nu + \nu_t) \left(\frac{\partial \bar{u}_i}{\partial x_j} + \frac{\partial \bar{u}_j}{\partial x_i} \right) \right] \quad (2)$$

where \bar{u}_i is the filtered velocity at the x_i direction, \bar{P} is the filtered pressure, and ν is the kinematic viscosity. ν_t is the eddy viscosity representing sub-grid stress, which is a space-dependent variable, unlike the kinematic viscosity that remains constant under constant temperature conditions. In this study, the coherent-structure model [15] was used to estimate the value of ν_t .

Furthermore, the computational domain was discretized using the collocated-grid approach, and the QUICK scheme [16] and the second-order accurate central finite difference were applied for the advection term and the other terms, respectively, of the spatial discretization to minimize the effects of numerical oscillation and numerical diffusion. For time discretization, the low-storage third-order Runge–Kutta scheme [17] was applied. It should be noted that, in this study, for the initial condition it was assumed that the working fluid completely filled the venous air trap chamber.

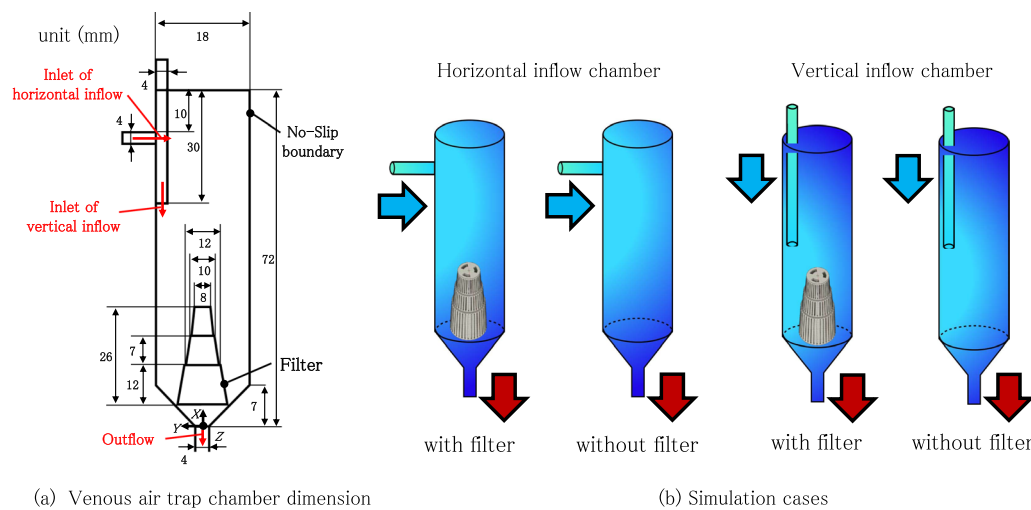


Fig. 1 Dimensions and design diagram of venous air trap chamber models. **a** Venous air trap chamber dimension. In the horizontal inflow chamber, the pipe (inflow pipe) entering the venous air trap chamber is horizontally attached. In the vertical inflow chamber, the pipe entering the venous air trap chamber is vertically inserted. The dimensions of the venous air trap chamber in this study were designed to be similar to those of a typical CRRT circuit. **b** Simulation cases. A total of four types of chambers were designed, including horizontal and vertical inflow chambers, each with and without filters. The capacity of each chamber was set to 15 ml

The numerical simulations in this study were performed using an in-house Fortran code developed by the authors. Extending the simulation time by one second would require approximately 150 days of computational effort using this code on a computer with an Intel Xeon E5-2667W or E5-2687W CPU, which limited our ability to test more variables.

Definition and discretization of computational domain (Grid Division)

In this study, the computational domain was the interior of the venous air trap chamber. Two types of inflow chambers, namely, horizontal and vertical inflow chambers, were designed for the inflow of the working fluid into the venous air trap chamber. We designed the venous air trap chamber on the basis of the blood circuit actually used in our hospital. The horizontal inflow chamber was referenced from the SUREFLOW N circuit (Nipro Inc, Osaka.), while the vertical inflow chamber was inspired by the CHDF-FSA circuit (Asahi Kasei Medical Inc, Tokyo.). Figure 1a shows the dimensions of the venous air trap chamber model designed in this study. These dimensions were chosen to be similar to those of a venous air trap chamber in a CRRT circuit used in actual clinical practice. As shown in Fig. 1b, the horizontal inflow chamber has an inflow pipe (inlet pipe) horizontally connected to the venous air trap chamber, while the vertical inflow chamber has an inflow pipe vertically connected to the venous air trap chamber. Four types of venous air trap chamber models were designed by considering the

conditions with and without a filter for both the horizontal and vertical inflow chambers (Fig. 1b). In all cases, the capacity of the venous air trap chamber was set to 15 ml.

Figure 2 shows the grid arrangement and dimension of the computational domain. The three-dimensional grids for the chamber (Fig. 2d) were generated by rotating the two-dimensional cross-section (Figs. 2a, b) around the x axis. The same computational domain was used for all the cases. For the grids regarded as the filter, the condition with a filter treated them as solid, while the condition without a filter treated them as fluid. Grids around the chamber wall and the filter were arranged more densely using hyperbolic tangent function (see Fig. 2), where the smallest grid space for the radial direction was set to be 0.08 mm.

The filter had three crescent-shaped slits on the top, each with a width of 1 mm and a length of approximately 2 mm. On the side, there were a total of 108 trapezoidal slits with dimensions (height, top base, bottom base) of 7, 0.26, and 0.29 mm; 7, 0.33, and 0.36 mm; and 12, 0.39, and 0.43 mm at the upper, middle, and lower parts, respectively. The area ratio of the inflow and outflow pipes of the venous air trap chamber was set to 1:1. Each defined computational domain was divided into $(200 \times 60 \times 289)$ grid points.

Numerical calculation and analysis/evaluation

From the computational results, streamlines of the flow field were illustrated to visualize the flow within the venous air trap chamber, representing the trajectories

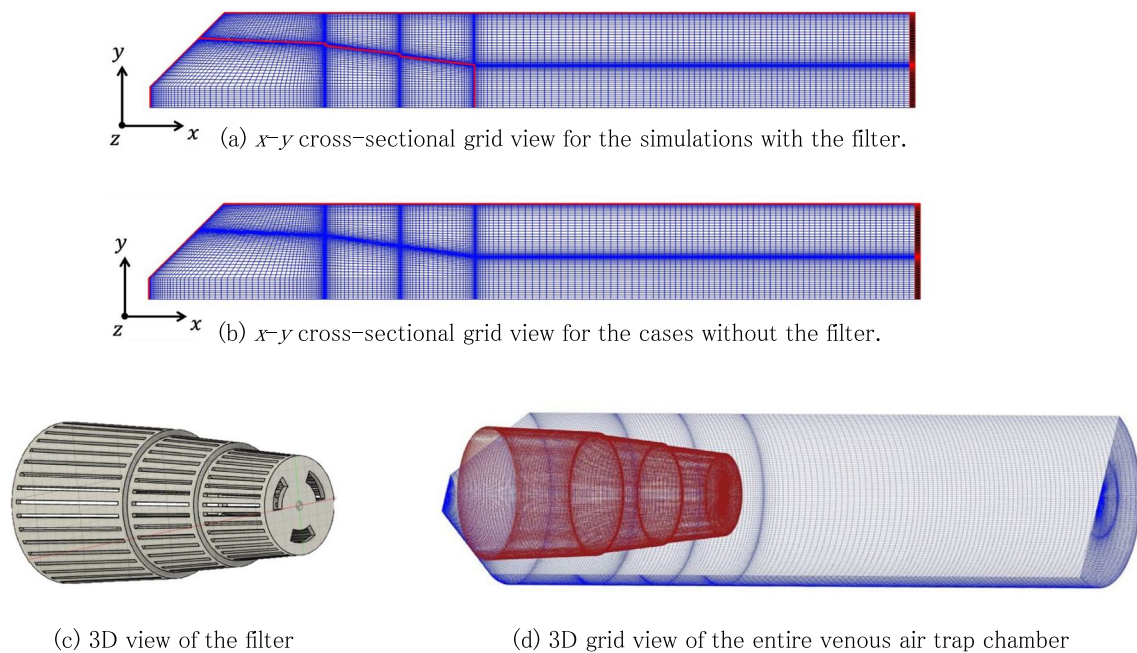


Fig. 2 Grid diagram used in CFD simulation. **a, b** x - y cross-sectional grid view for the simulations. Two types of grid diagrams were created, with and without filters. The blue grid represents the fluid, while the red regions indicate non-fluid areas. Attracting grid diagram with tanh function. Grid points: $200 \times 60 \times 289$. **c** Three-dimensional (3D) view of the filter. Upper gaps: semicircular sections (width 1 mm, length 2 mm) \times 3 locations. Side gaps: rectangular sections (width 0.3 mm) \times 108 locations. The gaps of the filter were set as fluid regions. **d** 3D grid view of the entire venous air trap chamber. For the generation of a three-dimensional grid in the computational domain, a two-dimensional grid was provided for one cross-section of the venous air trap chamber, which was then rotated to obtain the complete grid

of the flow. Velocity contours of the flow field were also depicted, showing the magnitude of velocity with colors.

In addition, the radial (R) distributions of the axial component of the average velocity (V_x) and turbulence intensity (V_{rms}) at six selected heights from the bottom of the chamber were visualized to investigate how the flow and its fluctuation change as it moves downstream. V_{rms} is calculated as the root-mean-square (rms) of the velocity differences from its mean value.

From the streamlines of the flow field, evaluations were made regarding the flow and vortex formation from the inlet to the outlet of the working fluid. Furthermore, the velocity distribution of the working fluid within the venous air trap chamber was visualized from the velocity contours of the flow field. In addition, based on the distribution of average velocity and turbulence intensity, we evaluated the degree of retention and flow variability within the venous air trap chamber. The combined analyses allowed the assessments of flow behaviors, such as stagnations.

In vitro experiments: visual evaluation of fluid flow in a venous air trap chamber

To validate the consistency of the results obtained from CFD simulations, experiments were conducted

in vitro. The blood circuits used in the in vitro experiments consisted of a horizontal inflow chamber: the SUREFLOW N circuit (Nipro Inc, Osaka.), and a vertical inflow chamber: the CHDF-FSA circuit (Asahi Kasei Medical Inc, Tokyo.), both featuring integrated filters. The SUREFLOW N circuit features a cone-type venous air trap chamber, while the CHDF-FSA circuit features a mesh-type. Initially, the chambers were modified by cutting the bottom of the chamber using an ultrasonic cutter (Honda Electronics Inc, Aichi.), followed by removing or not removing the filter and a rejoining of the chamber parts (Fig. 3). The volume of each chamber was adjusted to 15 ml, ensuring that all conditions were identical except for the presence or absence of the filter. The reservoir was filled with 1.5 L of 33% glycerin solution at 37°C and mixed with 10 ml of silver paint (Pentel Inc, Tokyo.) for visualization of flow in the venous air trap chamber. A recirculation experimental system was constructed in which both the arterial circuit and the vein circuit were connected to a water reservoir and circulated by a blood pump at a flow rate of 150 ml/min. The fluid flow in the venous air trap chamber was visually evaluated (Fig. 4).

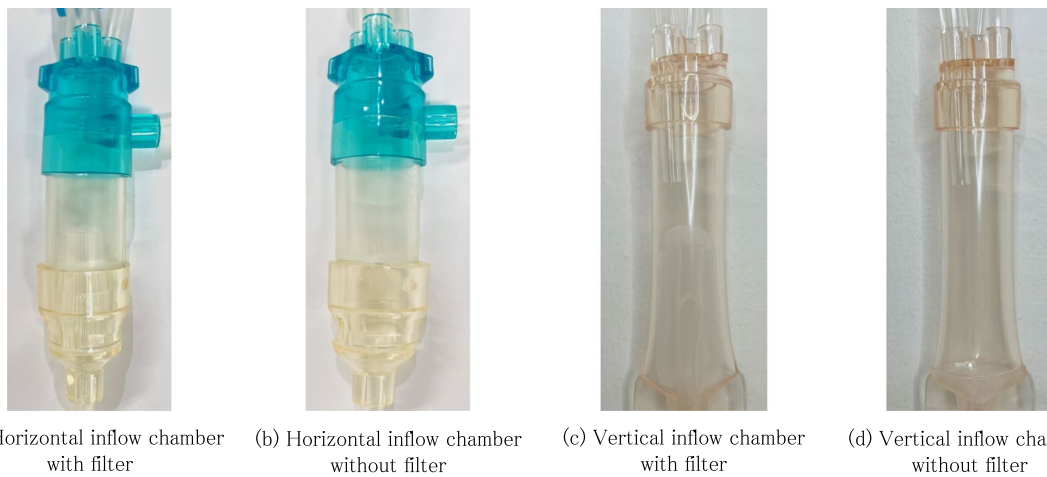


Fig. 3 The venous air trap chambers used in the in vitro experiments. The blood circuits used in the in vitro experiments consisted of a horizontal inflow chamber: the SUREFLOW N circuit, and a vertical inflow chamber: the CHDF-FSA circuit, both featuring integrated filters. Initially, the chambers were modified by cutting the bottom of the chamber using an ultrasonic cutter, followed by removing or not removing the filter and a rejoining of the chamber parts. The chamber volumes were adjusted to 15 ml

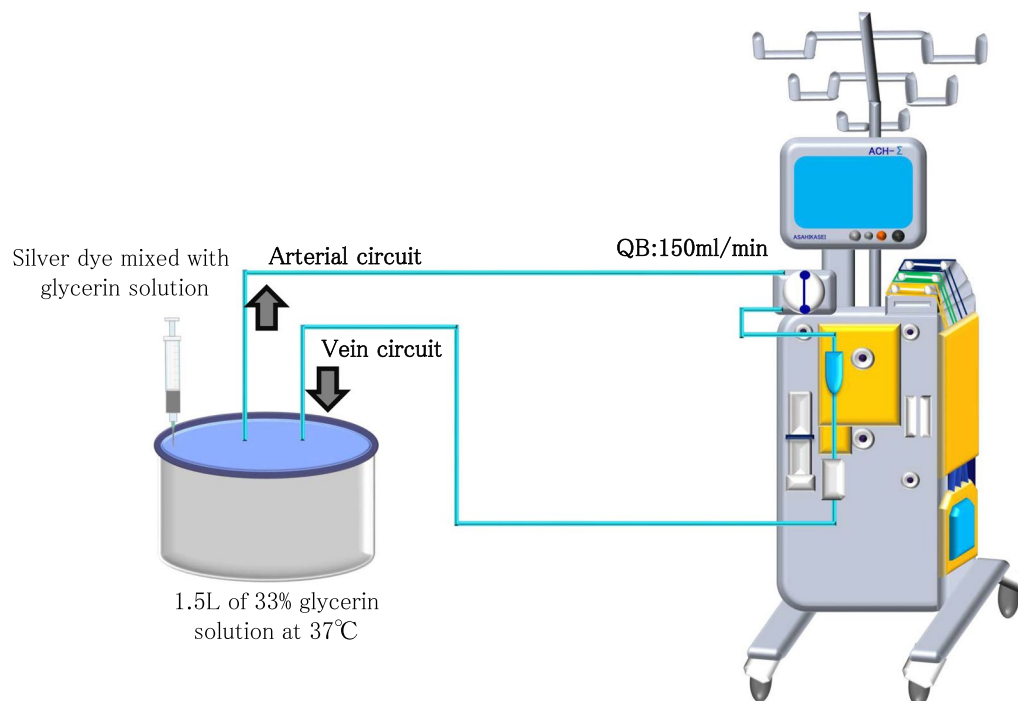


Fig. 4 In vitro evaluation method: visual evaluation of fluid flow in a venous air trap chamber. An experimental system was constructed in which both the arterial circuit and vein circuit were connected to a water reservoir, with a recirculating flow at a rate of 150 ml/min. The circulating fluid was 1.5 L of 33% glycerin solution at 37°C mixed with silver dye, and the fluid movement in the chamber was visually monitored

Results

CFD estimations of venous air trap chamber flow streams, in chamber models with or without filter and horizontal or vertical inflow (Fig. 1b), were as follows:

Horizontal inflow chamber with filter

From the streamlines of the flow field, it was observed that the working fluid, after inflow, splits in an upward and downward diagonal direction, ultimately flowing spirally downstream along the chamber walls. This vortex

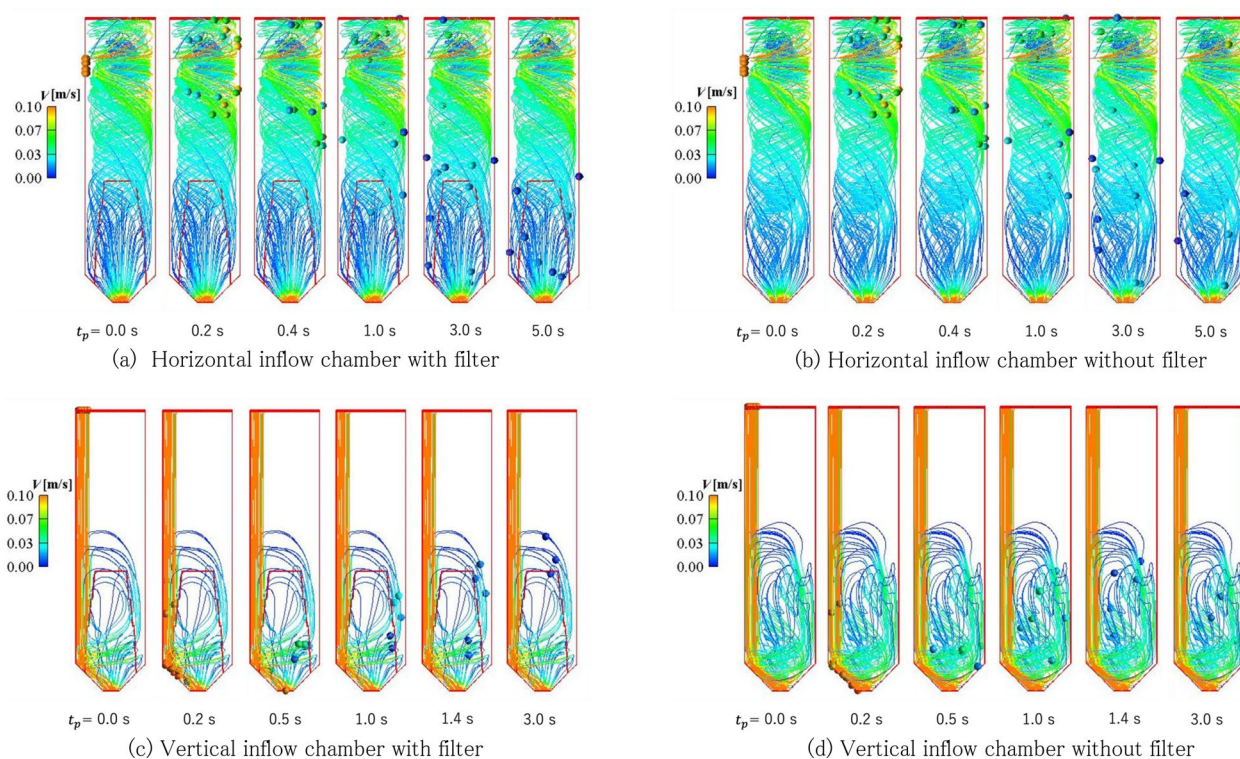


Fig. 5 CFD streamlines of the flow fields. In the horizontal inflow chamber **a, b**, irrespective of filter presence, the working fluid divided into upward and downward directions after inflow and ultimately flowed spirally along the chamber wall downstream. This vortex flow decreased as it flowed downstream. With the filter **(a)**, the working fluid uniformly flowed out from the filter, showing the streamlining effect of the filter. On the other hand, without the filter **b**, the flow was disturbed in the bottom part of the chamber. In the vertical inflow chamber **c, d**, irrespective of filter presence, the working fluid flowed vertically from the inlet into the main direction of the flow toward the outlet, but when reaching the bottom of the chamber part of the flow rebounded, and only after ascending and descending again, flowed out through the outlet. At positions higher than the inlet, streamlines diagrams were not drawn owing to stagnation. V : average flow velocity, t_p : elapsed time since the particle started moving, s : second

flow diminished as it progressed downstream, and, after passing through the filter, it uniformly exited from the filter. As evident from the streamlines of the flow field, the flow was rectified into a vortex-free flow (“potential flow” in fluid dynamics terminology) (Fig. 5a, Additional file 1a).

From the velocity contours of the flow field, it was determined that near the chamber walls in the upstream region where a vortex flow was formed, the flow velocity was faster compared with the center of the vortex flow. As the flow progressed downstream in the chamber, the flow velocity near the walls decreased, and the vortex flow was streamlined to a potential flow (Fig. 6a). The flow velocity near the filter was almost uniform. As is observed for the distribution of average velocity (Fig. 7a), the flow is directed toward the outlet at all the x positions, indicating that no backflow occurred in this condition. Moreover, the fluctuations of flow are observed to be negligibly small especially at the sections “1-3” where the filter is installed (Fig. 7b). These observations suggest

that the flow is streamlined by the filter, and there is no retention within the chamber.

In the *in vitro* experiments, it was confirmed that the fluid flowed in a swirling manner from the inlet to the outlet of the chamber without apparent stagnation (Additional file 2a).

Horizontal inflow chamber without filter

From the inlet to the filter section, both the streamlines and the velocity contours of the flow field showed similar results to those of the horizontal inflow chamber with filter, displaying predominantly a downward vortex flow (Figs. 5b, 6b, Additional file 1b). However, the flow dynamics at the chamber’s bottom showed less uniformity in both the streamlines and the velocity contours, and the flow did not streamline (potentiate) before reaching the outlet (Figs. 5b, 6b, Additional file 1b).

From the distributions of average velocity and turbulence intensity (Figs. 7a, b), it is revealed that the flow

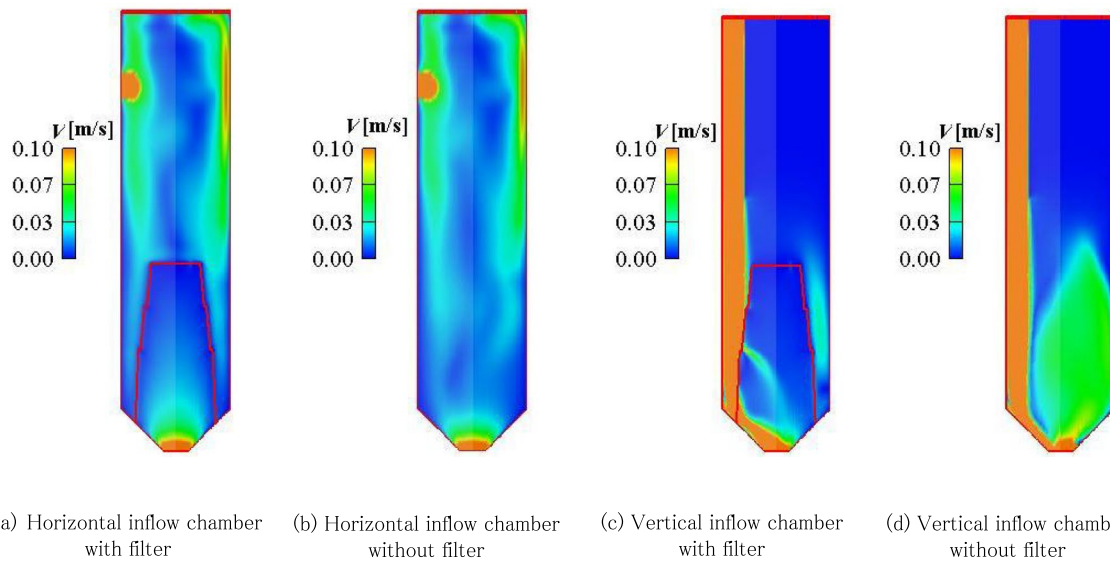


Fig. 6 Velocity contours of the flow fields. In the horizontal inflow chamber, irrespective of filter presence, a vortex flow was formed, with faster flow near the wall in the upper part of the chamber and slower flow at the center of the vortex. As the flow progressed downstream, the velocity near the wall decreased, and with the presence of a filter, the vortex flow was streamlined. In the vertical inflow chamber, irrespective of filter presence, it was observed that a portion of the incoming working fluid rebounded off the chamber bottom, causing flow reversal. The flow velocity at the top of the chamber was very low, leading to stagnation. Particularly in the vertical inflow chamber without a filter, significant bouncing off the chamber bottom was observed. V : average flow velocity

partly contains backflows near the chamber axis, and that the fluctuation is larger compared with the condition with a filter. This indicates that the flow is less streamlined compared with the the same inflow condition with filter.

Similar to the horizontal inflow with filter configuration, it was confirmed that the fluid flowed in a swirling manner from the inlet to the outlet of the chamber without apparent stagnation (Additional file 2b). In the in vitro experiments, detailed evaluation of fluid flow within the chamber could not be conducted as the assessment was done visually from outside the chamber, and this may be the reason why the streamlining effect of the filter could not be confirmed in the in vitro experiments.

Vertical inflow chamber with filter.

In the streamlines of the flow field, the working fluid flowed vertically from the inlet into the mainstream direction, with most of it flowing along the chamber wall and filtering directly toward the outlet (Fig. 5c). However, some of the working fluid bounced back at the bottom of the chamber and underwent upward and downward motions before flowing out to the outlet. Near the outlet, a streamlining effect of the flow owing to the filter was observed. No streamlines were depicted at positions higher than the inlet, representing stagnation (Fig. 5c, Additional file 1c).

In the velocity contour plot of the flow field, it was confirmed that most of the inflowing working fluid flowed directly to the outlet, while the flow velocity at the top of the chamber was found to be very low as a sign of stagnation (Fig. 6c).

The distribution of average velocity shows that the average velocities were high at the inflow side of the chamber where the working fluid vertically entered compared with the rest of the chamber (Fig. 7c). The distribution of turbulence intensity (Fig. 7d) reveals that the fluctuation was negligibly small. Therefore, it is concluded that in this chamber model the fluid is only in motion in a limited region and in the remaining of the chamber is mostly stagnant.

The in vitro experiments were consistent with these findings. The fluid bounced back at the bottom of the chamber and, after upward and downward motions, flowed out to the outlet. At the top of the chamber, no fluidity was observed, indicating fluid retention (Additional file 2c).

Vertical inflow chamber without filter

From the streamlines of the flow field, the working fluid flowed vertically from the inlet into the mainstream direction, with a part of it flowing directly along the chamber wall to the outlet (Fig. 5d, Additional file 1d). However, compared with the filtered condition, more of the working fluid bounced back at the bottom of the

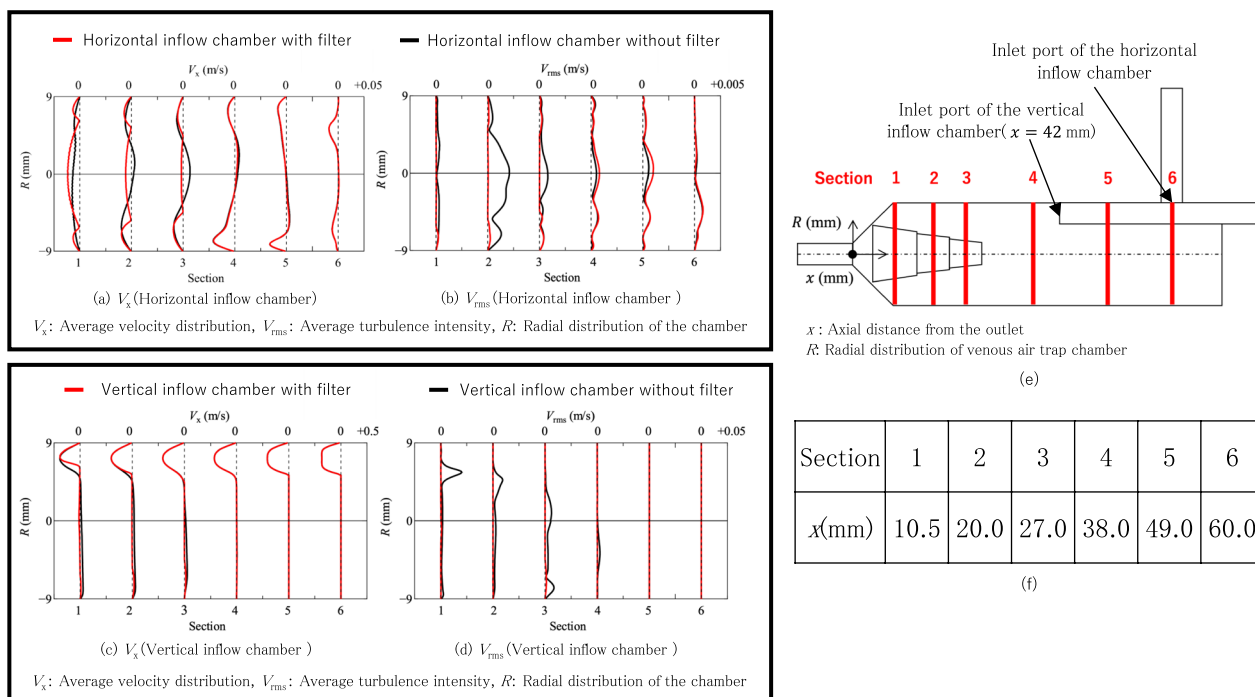


Fig. 7 The axial average flow velocity and turbulence intensity in the horizontal and vertical inflow configurations are compared. **a:** V_x (horizontal inflow chamber), **b:** V_{rms} (horizontal inflow chamber), **c:** V_x (vertical inflow chamber), **d:** V_{rms} (vertical inflow chamber), **e:** Schematic diagrams at each cross-sectional position and any position from the base of the chamber, **f:** axial distance from the outlet. From **a** and **c**, it is observed that the installation of a filter suppresses backflow. From **b** and **d**, it is evident that the turbulence intensity in the results with filters, for both horizontal and vertical inflow configurations, is smaller than that without filters, indicating a reduction in temporal flow fluctuations. Thus, in both chamber configurations, the installation of filters rectifies the flow. V_x : average velocity in the length direction of the chamber in m/s, V_{rms} : turbulence intensity in m/s, R : radial distribution of the chamber in mm, x : any position from the base of the venous air trap chamber. The cross-section numbers in the lower horizontal axes of Figs. 5a–d refer to their positions in Fig. 5e. The top horizontal axes in Fig. 5a and c are the scales for V_x with zeros representing zero velocity at each section and the graduations between two zeros indicating +0.05/−0.05 m/s (right/left from point zero); slightly differently presented are the top horizontal axes in Fig. 5 b and d where they indicate V_{rms} (which cannot be negative), with the scales for 0.01 and 0.05 m/s, respectively, being represented by the distance between the vertical line for the respective cross-section and the next vertical line (representing a cross-section or the top of the chamber) at the right thereof. The vertical axes show the radial distance R in mm from the chamber axis center for each cross-section (see also Fig. 1). Turbulence intensity is an indicator to express the extent of velocity fluctuations over time

chamber, underwent upward and downward motions similar to the condition with a filter, and only then flowed out to the outlet. Unlike in the filtered condition, the flow near the outlet was not rectified. As when using a filter, though, the streamline plots did not depict streamlines at the top of the chamber, indicating stagnation (Fig. 5d, Additional file 1d).

Similarly, in the velocity contour plot of the flow field, it was observed that the inflowing working fluid bounced back at the bottom of the chamber, while the flow velocity at the top of the chamber was very low, confirming stagnation (Fig. 6d).

Quite similar to as seen under the condition with filter, the average velocities were high at the side of the chamber where the working fluid vertically entered compared with the rest of the chamber (Fig. 7c). However, especially in cross-sections “1-3”, the turbulence

intensity distribution revealed large fluctuations that were not observed in the condition with filter (Fig. 7d). This fluctuation is due to the turbulence production generated by the large velocity gradient of jet flow at the inlet side. By contrast, the fluctuation was minimized in the case with the filter, owing to the streamlining of the flow.

In the in vitro experiments (Additional file 2d), similar fluid movements were observed as described above for the vertical inflow with filter configuration. Similar to the horizontal inflow chambers, detailed analyses and comparisons of the fluid movements within the vertical inflow chambers could not be conducted owing to visual assessment from outside the chamber. This may have contributed to the inability to confirm the streamlining effect of the filter in this in vitro experiment.

Discussion

In this study, we evaluated the effects of the differences in inlet configuration and the presence of filters on the flow dynamics within a venous air trap chamber by CFD simulations.

In horizontal inflow chamber models, irrespective of filter presence, the working fluid was found to flow smoothly without stagnation throughout the chamber, predominantly forming a vortex flow downstream along the chamber walls (Fig. 5a, b, Additional file 1a, b). It was observed that the flow velocity at the center of the vortex flow was lower than near the chamber wall, but without causing significant stagnation (Fig. 6a, b). In the numerical simulations of the horizontal inflow chamber, the effect of the filter is limited within the region where the filter is located and the flow is almost the same regardless of filter installation. However, the flow shows different patterns depending on whether it passes through the filter. After passing through the filter, the flow exhibits a potential flow pattern. On the other hand, in the absence of the filter, there is a slight vortex flow even in the lower part of the chamber (Figs. 5a, b, 6a, b). This streamlining effect by filter was confirmed by the distributions of average velocity and turbulence intensity (Fig. 7a, b).

By comparing Figs. 7a and c, it is observed that the flow when using the horizontal inflow method is streamlined better than when using the vertical inflow method. Additionally, it was observed that with the horizontal inflow configuration, the installation of the filter suppressed backflow, indicating a streamlining effect by the filter (Fig. 7a). Therefore, also in agreement with the streamline and velocity contour plots (Figs. 5a, b, 6a, b), it was evident that the filter prevents flow reversal and suppresses temporal fluctuations in velocity.

In the vertical inflow chamber, the incoming working fluid flowed vertically into the main flow direction. At the bottom of the chamber, a portion of the flow rebounded, and this behavior varied with the presence versus absence of a filter. In the presence of a filter, the majority of the incoming working fluid flowed along the chamber wall and filter toward the outlet. Some of the working fluid rebounded at the bottom of the chamber, there ascended from the outside of the filter, descended, passed through the filter, and then as a rectified flow ultimately exited the outlet (Figs. 5c, 6c). In the absence of the filter, most of the incoming working fluid strongly rebounded at the bottom of the chamber, and no potential flow was observed (Figs. 5d, 6d). Therefore, similar to the findings for the horizontal inflow chamber, the simulation results of the vertical inflow chamber also revealed a streamlining effect of the filter. Figure 7b and d demonstrate that, for both horizontal and vertical inflow methods, the turbulence intensity is lower in the filter installed cases. The

turbulence intensity where the filter is installed, both in the horizontal and vertical inflow chamber models, is smaller than that observed without filters at cross-sections including the filter position (cross-Sects “1-3” in Fig. 7). This concludes that the filter suppresses temporal flow fluctuations and that the installation of filters streamlines the flow.

As an additional observation, in the streamline plots results for the vertical inflow chamber, irrespective of filter presence, the rebounded flow only ascended to the vicinity of the inflow pipe outlet, and streamlines diagrams were not depicted in the upper part of the chamber, indicating stagnation (Fig. 5c, d). Two factors probably contributed to this: firstly, in the vertical inflow chamber, the working fluid enters from the middle portion of the venous air trap chamber, and secondly, the rebound at the bottom of the chamber does not extend to the top of the chamber.

On the basis of the results obtained from the numerical fluid simulations, the flow from the inlet to the outlet was relatively smooth in the “vertical inflow chamber with filter” configuration (Figs. 5c, 6c). However, since the flow velocity at the top of the chamber was very low and stagnation occurred, it is concluded that this chamber design does not ensure a completely smooth flow throughout the venous air trap chamber (Figs. 5c, 6c). On the other hand, in the horizontal inflow chamber, the flow remained smooth throughout the venous air trap chamber, characterized by the formation of vortex flow (Figs. 5a, b, 6a, b). Additionally, the presence of a filter helped streamline the flow toward the outlet (Figs. 5a, 6a), supporting that the “horizontal inflow chamber with filter” design promotes a smooth flow throughout the venous air trap chamber.

In addition, *in vitro* experiments with conditions matching the CFD simulations were conducted to validate the computational results. In these *in vitro* experiments, the fluid flow near the outer wall of the venous air trap chamber was visually evaluated. It should be noted that, unlike the CFD analysis, these experiments were effective only for qualitative assessment. The overall fluid flow patterns observed in the experiments agreed with the CFD analysis results for both horizontal and vertical inflow cases, with stagnation only observed in the latter (Additional file 2). However, differences in flow patterns owing to the presence or absence of the filter could not be observed in the *in vitro* experiments. Whether similar patterns were fully absent or were too subtle to be detectable by our *in vitro* method, remains to be determined. In the future, we may also need to evaluate parameters that could cause differences between the experimental filter and our CFD concept of the filter.

We have previously performed in vitro experiments using a CRRT machine commonly used in clinical practice and reported for a venous air trap chamber with horizontal inflow and without filter that the fluid flows smoothly [18]. Filters integrated into a venous air trap chamber serve to remove air bubbles and clots; however, they also impede flow, which may lead to fluid retention and stagnation within the chamber [3]. Therefore, we had assumed that removing the filter from the venous air trap chamber would help mitigate the occurrence of retention and stagnation. However, the results of the numerical fluid simulation in this study revealed that the filter does not contribute to flow irregularities, but, instead, streamlines the flow. From the perspective of achieving stagnation-free flow, it appears that, at least in theory, having a filter integrated into the venous air trap chamber has beneficial effects. To demonstrate the beneficial effects of the filter in a more practical setting, experiments will be necessary that, for example, analyze the correlation of the presence or absence of the filter with the time until blood coagulation occurs. Therefore, we cannot determine yet whether incorporating the filter into the venous air trap chamber will have a beneficial outcome for the patient.

Two of the major reasons for the differences between our previous in vitro results [18] and the here presented CFD analysis are the experimental models used (in vitro experiments versus numerical simulations) and the nature of fluid flow (pulsatile flow versus steady flow). In clinical practice, CRRT devices utilize roller pumps for extracorporeal circulation. Owing to the characteristics of roller pumps, the fluid flows through the blood circuit as pulsatile flow and eventually enters the venous air trap chamber. In the present study, however, to simplify the numerical calculations, the operating fluid was defined to enter the venous air trap chamber as a steady flow. Additionally, while the dimensions of the venous air trap chamber used in this numerical simulation were designed to be similar to those of the venous air trap chamber in CRRT circuits used in clinical practice, they were not exactly the same as those used in the in vitro experiments.

There are several limitations of the present study that cause uncertainty of whether the results can be directly applied to the clinical practice. Firstly, in the future, further numerical fluid simulations that take into account the characteristics of pulsatile flow are necessary to bring the study closer to clinical relevance. Secondly, in this study, the numerical calculations were performed considering the viscosity of a 33% glycerin solution instead of blood. Therefore, the behavior of actual blood should be addressed in future studies. Thirdly, in our numerical calculations, a conical filter was adopted for simplification purposes. Since mesh-type filters are

commonly used as well, additional studies employing mesh-type filters should be conducted. Fourth, in this study, the flow rate of the working fluid was set at 150 ml/min, because in our ICU, the blood flow rate during CRRT is typically set at 150 ml/min. However, in other clinics, the preferred flow rate may be different, and if in our CFD models the flow rates of the working fluid would be changed, different results might be obtained. Fifthly, since this study did not investigate the “effectiveness of the filter and inhibition of blood coagulation,” it remains unclear whether incorporating the filter into the venous air trap chamber will yield beneficial effects. Therefore, it is necessary to conduct experiments correlating the “effectiveness of the filter and inhibition of blood coagulation” in future studies. Sixth, the difference in the type of the venous air trap chamber filter used in the in vitro experiments. In this study, the analysis was conducted assuming a cone-type filter. Therefore, ideally, cone filters should have been used for the in vitro experiments. However, our hospital only employs the SUREFLOW N circuit with a cone-type filter for the horizontal inflow chamber blood circuit and the CHDF-FSA circuit with a mesh-type filter for the vertical inflow chamber blood circuit. Owing to the inability to conduct in vitro experiments with venous air trap chambers of the same shape and type of filter, there is a possibility that the in vitro experiments do not accurately represent the validity of the CFD analysis results. In the future, we aim to create venous air trap chambers with identical shapes and conduct further detailed CFD analysis. Despite of the limitations above, as described in the earlier sections, the present CFD analysis reproduced the flows in the air trap venous chamber in a qualitative manner because both experimental and numerical results show the flows in a swirling motion. The use of other experimental techniques, including particle image velocimetry (PIV), is effective for the quantitative evaluation.

Conclusions

We estimated, by using CFD analysis, the influence of different chamber designs on the flow within the venous air trap chamber in a CRRT circuit. By numerical fluid simulations the “horizontal inflow chamber with filter” was identified as the venous air trap chamber design that promoted a smooth flow throughout the chamber.

Abbreviations

CRRT	Continuous renal replacement therapy
CFD	Computational fluid dynamics
CFD analysis	Computational fluid dynamics analysis
LES	Large eddy simulation

Supplementary Information

The online version contains supplementary material available at <https://doi.org/10.1186/s41100-024-00569-5>.

Additional file 1. Animations of particles following the streamlines of the flow fields. Animations were created of particles flowing along the streamlines obtained by numerical analysis. In the horizontal inflow chamber, irrespective of filter presence, the working fluid divided into upward and downward directions after inflow and ultimately flowed spirally downstream along the chamber wall. This vortex flow decreased as it flowed downstream. With the filter, the working fluid uniformly flowed out from the filter, showing the streamlining effect of the filter. On the other hand, without the filter, the flow was disturbed in the bottom part of the chamber. In the vertical inflow chamber, irrespective of filter presence, the working fluid flowed vertically from the inlet into the main direction of flow, then rebounded at the bottom of the chamber, and after ascending and descending again, flowed out through the outlet. Additionally, at positions higher than the inlet, streamline plots were not drawn due to stagnation.

Additional file 2. In vitro experiments: Visual evaluation of fluid in a venous air trap chamber. In the horizontal inflow chamber, it was confirmed that the fluid flows uniformly throughout the chamber as a vortex flow regardless of the presence of the filter. Additionally, no retention was observed in the horizontal inflow chamber. In the vertical inflow chamber, we observed a non-uniform motion of fluid winding pulsatilely upward from the bottom of the chamber. In addition, there was no fluidity in the upper layer of the liquid surface, and stagnation occurred. Also here, visually we could not conclude a difference caused by the presence or absence of the filter.

Acknowledgements

We thank Dr. Johannes M. Dijkstra of the Office of Research Administration, Fujita Health University, for the English proofreading of our article.

Author contributions

KS wrote the manuscript and analyzed the data; TY, CK, and YM designed the study and revised the manuscript; CH, NK, YH, TK, and SK contributed to data collection; KM, TY, YM, ON, and TN discussed the results and contributed to the final manuscript. All authors read and approved the final manuscript.

Funding

We have no sources of funding to declare for this manuscript.

Availability of data and materials

The authors declare that the data supporting the findings of this study are available within the paper and its Supplementary Information files. Should any raw data files be needed in another format they are available from the corresponding author upon reasonable request.

Declarations

Conflict of interest

Not applicable.

Ethics approval and consent to participate

This study does not involve human or animal subjects, so ethical considerations are not applicable.

Consent for publication

This study does not involve human or animal subjects, so ethical considerations are not applicable.

Author details

¹Department of Clinical Engineering, Fujita Health University Hospital, Toyoake, Aichi, Japan. ²Graduate School of Engineering, Nagoya Institute of Technology, Nagoya, Aichi, Japan. ³Laboratory for Immune Response and Regulatory Medicine, Fujita Health University School of Medicine, 1-98 Dengakugakubo, Kutsukake-Cho, Toyoake, Aichi 470-1192, Japan.

⁴Department of Anesthesiology and Critical Care Medicine, Fujita Health University School of Medicine, Toyoake, Aichi, Japan.

Received: 6 April 2024 Accepted: 24 August 2024

Published online: 12 September 2024

References

- Jonsson P, Stegmayr C, Stegmayr B, et al. Venous chambers in clinical use for hemodialysis have limited capacity to eliminate microbubbles from entering the return bloodline: an in vitro study. *Artif Organs*. 2023;47:961–70.
- Jonsson P, Karlsson L, Forsberg U, et al. Air bubbles pass the security system of the dialysis device without alarming. *Artif Organs*. 2007;31:132–9.
- Baldwin I. Factors affecting circuit patency and filter "life." *Contrib Nephrol*. 2007;156:178–84.
- Baldwin I, Fealy N, Carty P, et al. Bubble chamber clotting during continuous renal replacement therapy: vertical versus horizontal blood flow entry. *Blood Purif*. 2012;34:213–8.
- Shin J, Song HC, Hwang JH, et al. Impact of downtime on clinical outcomes in critically ill patients with acute kidney injury receiving continuous renal replacement therapy. *ASAIO J*. 2021;68:744–52.
- Uchino S, Fealy N, Baldwin I, Morimatsu H, Bellomo R. Continuous is not continuous: the incidence and impact of circuit "down-time" on uraemic control during continuous veno-venous haemofiltration. *Intensive Care Med*. 2003;29:575–8.
- Cutts MW, Thomas AN, Kishen R. Transfusion requirements during continuous veno-venous haemofiltration: the importance of filter life. *Intensive Care Med*. 2000;26:1694–7.
- Torabi A, Dehkordi MAS. Using computational fluid dynamics for hemodialysis air chamber design modification. *J Artif Organs*. 2022;45(5):488–96.
- Shimazaki N, Ishigaki H, Okuno T, et al. Computational fluid dynamics analysis for proposing optimized chamber configurations to suppress blood coagulation. *Toin Univ Yokohama Res Bull*. 2023;48:79–84.
- Fletcher CAJ. *Computational techniques for fluid dynamics 1: fundamental and general techniques*. Springer-Verlag, Berlin; 1988.
- Kamada H, Nakamura M, Ota H, Higuchi S, Takase K. Blood flow analysis with CFD and 4D-flow MRI for vascular diseases. *J Cardiol*. 2022;80(5):386–96.
- Brookshier KA, Tarbell JM. Evaluation of a transparent blood analog fluid: aqueous xanthan gum/glycerin. *Biorheology*. 1993;30(2):107–16.
- Wells RE Jr, Merrill EW. Influence of flow properties of blood upon viscosity-hematocrit relationships. *J Clin Invest*. 1962;41(8):1591–8.
- Segur JB, Oberstar HE. Viscosity of glycerol and its aqueous solutions. *Ind Eng Chem*. 1951;43(9):2117–20.
- Kobayashi H. The subgrid-scale models based on coherent structures for rotating homogeneous turbulence and turbulent channel flow. *Phys Fluids*. 2005;17(4):045104.1–045104.12.
- Leonard BP. A stable and accurate convective modelling procedure based on quadratic upstream interpolation. *Comput Methods Appl Mech Eng*. 1979;19(1):59–98.
- Spalart PR, Moser RD, Rogers MM. Spectral methods for the Navier-Stokes equations with one infinite and two periodic directions. *J Comput Phys*. 1991;96:287–324.
- Shimizu K, Moriyama K, Kuriyama N, et al. Differences in chamber structure contribute to the incidence of venous air trap chamber coagulation during AN69ST-CHF: clinical and in vitro evaluation. *Ren Replace Ther*. 2024;10:10.

Publisher's Note

Springer Nature remains neutral with regard to jurisdictional claims in published maps and institutional affiliations.